



HAL
open science

A multivariate CUSUM control chart for monitoring Gumbel's bivariate exponential data

Fupeng Xie, Jinsheng Sun, Philippe Castagliola, Xuelong Hu, Anan Tang

► **To cite this version:**

Fupeng Xie, Jinsheng Sun, Philippe Castagliola, Xuelong Hu, Anan Tang. A multivariate CUSUM control chart for monitoring Gumbel's bivariate exponential data. *Quality and Reliability Engineering International*, 2021, 37 (1), pp.10-33. 10.1002/qre.2717 . hal-03112644

HAL Id: hal-03112644

<https://hal.science/hal-03112644>

Submitted on 24 Jun 2021

HAL is a multi-disciplinary open access archive for the deposit and dissemination of scientific research documents, whether they are published or not. The documents may come from teaching and research institutions in France or abroad, or from public or private research centers.

L'archive ouverte pluridisciplinaire **HAL**, est destinée au dépôt et à la diffusion de documents scientifiques de niveau recherche, publiés ou non, émanant des établissements d'enseignement et de recherche français ou étrangers, des laboratoires publics ou privés.

A Multivariate CUSUM Control Chart for Monitoring Gumbel's Bivariate Exponential Data

FuPeng Xie¹, JinSheng Sun¹, Philippe Castagliola², XueLong Hu^{*3} and AnAn Tang³

¹*School of Automation, Nanjing University of Science and Technology, Nanjing, China*

²*Université de Nantes & LS2N UMR CNRS 6004, Nantes, France*

³*School of Management, Nanjing University of Posts and Telecommunications, Nanjing, China*

Abstract

Exponential distributed data are commonly encountered in high-quality processes. Control charts dedicated to the univariate exponential distribution have been extensively studied by many researchers. In this paper, we investigate a Multivariate Cumulative Sum (MCUSUM) control chart for monitoring Gumbel's Bivariate Exponential (GBE) data. Some tables are provided to determine the optimal design parameters of the proposed MCUSUM GBE chart. Furthermore, both zero- and steady-state properties of the proposed MCUSUM GBE chart are compared with the multivariate exponentially weighted moving average (MEWMA) chart and the paired individual Cumulative Sum (CUSUM) chart. The results show that the proposed MCUSUM GBE chart outperforms the other two types of control charts for most shift domains. In addition, an illustrative example is provided in order to explain how the proposed MCUSUM GBE chart can be implemented in practice.

Keywords: Multivariate CUSUM chart; Gumbel's Bivariate Exponential distribution; Average Run Length.

1 Introduction

As one of the most important on-line monitoring technique, control charts have been widely used to detect assignable causes in manufacturing industries¹. For high-quality processes, the occurrences of defects or nonconformities are very low, say, parts per million (ppm) or even parts per billion (ppb), which make the traditional charts, like the p and np charts, facing many practical issues (like, for example, a high probability of false alarm, control limits that are meaningless and a low efficiency in the detection of shifts), see Xie et al.².

Differing from the traditional control charts, TBE (Time-Between-Event) charts are well-known for monitoring the time between successive occurrences of a specific event. Most studies on univariate TBE type charts are based on the assumption that the occurrences of this event follow a homogeneous Poisson process, i.e., the time between two successive events follows an exponential distribution, see Chan et al.³, Liu et al.⁴ and Liu et al.⁵. In addition, TBE type charts for monitoring the gamma,

*CONTACT: XueLong Hu. Email: hxl0419@hotmail.com

the lognormal or the Weibull distributions are also common, readers can refer for instance to Zhang et al.⁶, Zhang and Chen⁷, Rahali et al.⁸ and Wang et al.⁹.

By definition, univariate control charts focus on processes which only have a single quality characteristic of interest. But, in practice, there are many situations where several related quality characteristics of interest need to be monitored simultaneously. Using several univariate control charts to separately monitor these quality characteristics is known to be ineffective and misleading, because of the natural correlation between the quality characteristics. Therefore, multivariate control charts are suggested to monitor all the quality characteristics together. The original work on multivariate control charts for the mean vector has been proposed by Hotelling¹. After that, many other multivariate control charts have been proposed, including the multivariate cumulative sum (MCUSUM) charts (see Crosier¹⁰, Pignatiello Jr and Runger¹¹) and the multivariate exponentially weighted moving average (MEWMA) charts (see Lowry et al.¹²). It is worth noting that these control charts all assume multivariate normality for the data.

In the case of high-quality processes, univariate and multivariate TBE data usually follow a non-normal and highly skewed distribution. Using traditional multivariate control charts (as the ones cited above) that assume multivariate normality may result in a poor detection power when monitoring TBE data. Various approaches have been proposed in the literature to monitor non-normal distributed data. Among them, some nonparametric control charts have been proposed to monitor univariate and multivariate skewed populations, see Zou and Tsung¹³, Tang et al.¹⁴, Zhou et al.¹⁵ and Yue and Liu¹⁶.

Although attractive, these nonparametric control charts are difficult to apply in practice due to the expensive computations required for their implementation. On the other hand, with the help of some data transformations, a multivariate non-normal distribution can be approximately transformed into a multivariate normal distribution or into the combination of different normal distributions, for example, using the double square-root method (see Kittlitz Jr¹⁷) or the weighted standard deviation method (see Chang and Bai¹⁸ and Chang¹⁹). Because data transformation may lead to some loss of useful information, it should be carefully considered as an appropriate method for process monitoring. In addition, Stoumbos and Sullivan²⁰ and Testik et al.²¹ showed that the MEWMA control chart with a small smoothing parameter is fairly robust to the non-normality assumption. Based on this remark, Xie et al.²² investigated the properties of the MEWMA chart for monitoring the mean shift vector of a Gumbel's Bivariate Exponential (GBE) distribution²³. The results showed that the MEMWA chart is superior to the paired individual t chart² and the paired individual EWMA chart for both raw and transformed data.

The performance of univariate or multivariate control charts is usually measured by the ARL (Average Run Length), which is defined as the average number of observations required for the chart to give a signal. If a shift occurs in the process as soon as the monitoring begins or when the chart statistic is at its initial value, the ARL is called the *zero-state* ARL. But, in practice, there is no reason to assume that some shift exactly occurred in the process when the process monitoring started. Instead, it is usually assumed that some random shifts occur after a period of in-control time and the ARL obtained this way is called the *steady-state* ARL. In many situations, the steady-state ARL performance of a control chart is more informative than its zero-state counterpart. Khoo²⁴ and Szarka III and Woodall²⁵ used the steady-state ARL performance as the metric to evaluate the performance of different control charts. Recently, Knoth²⁶ derived the steady-state and the worst-case ARLs of the MEWMA chart using exact integral equations.

It is known that there are many similarities between the MEWMA and the MCUSUM charts (see Chang¹⁹, Lowry and Montgomery²⁷). Both of them use the information from historical observations, which makes these two charts more sensitive to detect small shifts in the process. If monitoring Gumbel's Bivariate Exponential data with a MEWMA control chart has already been investigated in Xie et al.²², as far as we know, no research has been conducted on (a) proposing a MCUSUM type control chart for monitoring such data and (b) evaluating zero- and steady-state performances of this chart for a direct comparison with its MEWMA counterpart.

In this paper, we investigate the properties of the MCUSUM chart for monitoring data having a GBE distribution. In Section 2, the GBE model is first introduced, and then the MCUSUM chart monitoring GBE distributed data is presented. In Section 3, the steps for the computation of both in- and out-of-control zero- and steady-state ARLs are detailed. Then in Section 4, a numerical comparison is performed between the proposed MCUSUM GBE chart and the MEWMA and paired individual CUSUM charts in the case of downward, upward and hybrid shifts. In addition, some guidelines for constructing the MCUSUM GBE chart are also provided. In Section 5, an illustrative example is provided in order to demonstrate the use of the proposed MCUSUM GBE chart on monitoring patient headache relief time. Finally, some conclusions complete the paper in Section 6.

2 The MCUSUM chart for Bivariate Exponential data

2.1 Gumbel's Bivariate Exponential model

The bivariate exponential model used in this paper was firstly introduced by Gumbel²³ and named as the GBE model. If (X_1, X_2) are the random variables of the standard GBE model, then $(X_1, X_2) \in \mathbb{R}^+$ and their joint survival function is,

$$\bar{F}_{X_1, X_2}(x_1, x_2) = \exp\left(-\left(x_1^{\frac{1}{\delta}} + x_2^{\frac{1}{\delta}}\right)^\delta\right), \quad (1)$$

where $\delta \in (0, 1]$ is the dependence parameter. It is noted that if $\delta = 1$, X_1 and X_2 are uncorrelated. Otherwise ($\delta \neq 1$), X_1 and X_2 are correlated.

Lu and Bhattacharyya²⁸ introduced a more general expression for the GBE model,

$$\bar{F}_{X_1, X_2}(x_1, x_2) = \exp\left(-\left(\left(\frac{x_1}{\theta_1}\right)^{\frac{1}{\delta}} + \left(\frac{x_2}{\theta_2}\right)^{\frac{1}{\delta}}\right)^\delta\right), \quad (2)$$

where $\theta_1 > 0$ and $\theta_2 > 0$ are two scale parameters. The p.d.f (probability density function) of the general GBE model is,

$$f_{X_1, X_2}(x_1, x_2) = (\theta_1 \theta_2)^{-\frac{1}{\delta}} (x_1 x_2)^{\frac{1}{\delta}-1} \left(\left(\frac{x_1}{\theta_1}\right)^{\frac{1}{\delta}} + \left(\frac{x_2}{\theta_2}\right)^{\frac{1}{\delta}}\right)^{\delta-2} \left(\left(\left(\frac{x_1}{\theta_1}\right)^{\frac{1}{\delta}} + \left(\frac{x_2}{\theta_2}\right)^{\frac{1}{\delta}}\right)^\delta + \frac{1}{\delta} - 1\right) \times \exp\left(-\left(\left(\frac{x_1}{\theta_1}\right)^{\frac{1}{\delta}} + \left(\frac{x_2}{\theta_2}\right)^{\frac{1}{\delta}}\right)^\delta\right). \quad (3)$$

From the joint survival function of the GBE model, it is easy to prove that the marginal distribution of X_1 and X_2 is the exponential distribution of parameter θ_1 and θ_2 , respectively. Therefore, the mean vector $\boldsymbol{\mu}$ of $(X_1, X_2)^\top$ is equal to,

$$\boldsymbol{\mu} = \begin{pmatrix} \theta_1 \\ \theta_2 \end{pmatrix}, \quad (4)$$

and its variance-covariance matrix $\boldsymbol{\Sigma}$ is,

$$\boldsymbol{\Sigma} = \begin{pmatrix} \theta_1^2 & \rho\theta_1\theta_2 \\ \rho\theta_2\theta_1 & \theta_2^2 \end{pmatrix}, \quad (5)$$

where the coefficient of correlation ρ is (see Lu and Bhattacharyya²⁸),

$$\rho = \frac{2\Gamma^2(\delta + 1)}{\Gamma(2\delta + 1)} - 1, \quad (6)$$

and where $\Gamma(\dots)$ is the gamma function.

2.2 The MCUSUM chart for the GBE model

Among the multivariate CUSUM charts that have been proposed, the one proposed by Crosier¹⁰ for multivariate normal data (as a natural extension of the two-sided CUSUM chart also introduced by Crosier²⁹) is probably the most widely used. In this paper, we adapt Crosier's¹⁰ MCUSUM chart in the case of GBE data.

Suppose that $\mathbf{X}_t = (X_{1,t}, X_{2,t})^\top$ is a random vector observed at regular sampling time $t = 1, 2, \dots$. According to Crosier¹⁰, the MCUSUM statistic \mathbf{S}_t is defined as,

$$\mathbf{S}_t = \begin{cases} \mathbf{0}, & \text{if } C_t \leq k, \\ (\mathbf{S}_{t-1} + \mathbf{X}_t - \boldsymbol{\mu}_0) \left(1 - \frac{k}{C_t}\right), & \text{if } C_t > k, \end{cases} \quad (7)$$

with

$$C_t = ((\mathbf{S}_{t-1} + \mathbf{X}_t - \boldsymbol{\mu}_0)^\top \boldsymbol{\Sigma}^{-1} (\mathbf{S}_{t-1} + \mathbf{X}_t - \boldsymbol{\mu}_0))^{\frac{1}{2}}, \quad (9)$$

where $\boldsymbol{\mu}_0 = (\theta_1, \theta_2)^\top$ is the in-control mean vector, $\boldsymbol{\Sigma}$ is the in-control variance-covariance matrix as defined in (5) and (6), the process initial statistic $\mathbf{S}_0 = \mathbf{0}$ and $k > 0$ is a reference parameter. An out-of-control signal is given when the statistic $Q_t = (\mathbf{S}_t^\top \boldsymbol{\Sigma}^{-1} \mathbf{S}_t)^{\frac{1}{2}} > H$, where $H > 0$ is the upper control limit of the MCUSUM GBE chart.

In order to evaluate the Run Length (RL) properties of the proposed MCUSUM GBE chart, the following Monte-Carlo type procedure will be used:

Step 1: Specify the design parameters k and H , the scale parameters θ_1 and θ_2 and the dependence parameter δ of the GBE model.

Step 2: Generate the random variables $X_{1,t}$ and $X_{2,t}$ of the GBE model at time $t = 1, 2, \dots$ using the following equations²⁸,

$$E = E_1 + \Psi E_2, \quad (10)$$

$$X_{1,t} = \theta_1 U^\delta E, \quad (11)$$

$$X_{2,t} = \theta_2 (1 - U)^\delta E, \quad (12)$$

where U , E_1 , E_2 and Ψ are four independent random variables such that U is a uniform $(0, 1)$ random variable, E_1 and E_2 are two exponential random variables both with scale parameter $\theta_E = 1$, and $\Psi \in \{0, 1\}$ is a Bernoulli random variable with parameter δ (the dependence parameter), i.e., $P(\Psi = 0) = 1 - \delta$ and $P(\Psi = 1) = \delta$.

Step 3: Calculate the MCUSUM statistic \mathbf{S}_t at time $t = 1, 2, \dots$, using (7), (8) and (9).

Step 4: If the statistic $Q_t = (\mathbf{S}_t^T \boldsymbol{\Sigma}^{-1} \mathbf{S}_t)^{\frac{1}{2}} > H$, the process is deemed to be out-of-control, and the corresponding RL value is recorded.

Step 5: Repeat Steps (2)-(4) to obtain 5×10^4 RL values and estimate the required RL properties like, for instance, the ARL, the MRL, the SDRL or any quantiles of the RL. In this paper, we will focus of the ARL.

For the proposed MCUSUM GBE chart, an acceptable in-control ARL (ARL_0) is specified at the beginning of the process monitoring, and the aim of the chart is to obtain the minimum out-of-control ARL (ARL_1) value for a predetermined mean shift. In order to achieve the desired ARL_0 , combinations of the reference parameter k and the corresponding control limit H of the proposed MCUSUM GBE chart need to be determined first. Once the reference parameter k and the dependency parameter δ are fixed, the approximate H value can be obtained using the constraint on the desired ARL_0 . More details about the ARL performance of the proposed MCUSUM GBE chart are described in the next section.

3 Average Run Length of the MCUSUM GBE chart

For the proposed MCUSUM GBE chart, an acceptable in-control ARL_0 is chosen, and the smaller the out-of-control ARL_1 , the better the performance of the control chart. In this paper, the in- and out-of-control processes are modeled by a $GBE(\theta_1, \theta_2, \delta)$ and a $GBE(\theta'_1, \theta'_2, \delta)$, respectively, keeping the dependence parameter δ unchanged. Moreover, both zero- and steady-state ARL performances of the proposed MCUSUM GBE chart are analyzed.

3.1 Zero-state case

The zero-state ARL performance is one of the most widely used criterion for control charts. It is based on the assumption that a sustained shift in the parameter occurs upon startup or that the chart statistic is at its initial starting value when the shift in the parameter occurs³⁰.

Similar to the Appendix A in Xie et al.²², it can be proven that, when the design parameters k and H are determined and the dependency parameter δ remains constant, the ARL performance of the proposed MCUSUM GBE chart only depends on the mean shift vector (τ_1, τ_2) , where $\tau_1 = \theta'_1/\theta_1$ and $\tau_2 = \theta'_2/\theta_2$ are the variables quantifying the shift. Therefore, in the zero-state case, we keep the dependency parameter δ as a constant, and set the mean shift vector $(\tau_1, \tau_2) = (1, 1)$ to denote the in-control process.

In the zero-state case, the procedure for determining the optimal design parameters k and H of the proposed MCUSUM GBE chart can be described as follows:

- Step 1: Specify the desired ARL_0 value, the dependency parameter δ and the mean shift vector of interest (τ_1, τ_2) .
- Step 2: For different values of the reference parameter $k \in \{0.02, 0.05, 0.07, 0.1, 0.2, 0.3, 0.4, 0.5, 0.6, 0.7, 0.8, 0.9, 1, 3\}$, find the corresponding control limit H of the MCUSUM GBE chart satisfying the desired ARL_0 . For example, Table 1 shows the combinations of design parameters k and H leading to the desired $ARL_0 \in \{100, 200, 370\}$ when the dependency parameter $\delta \in \{0.2, 0.5, 0.7, 0.9\}$.
- Step 3: For the mean shift vector of interest (τ_1, τ_2) and different combinations of k and H specified in Step (2), calculate the corresponding out-of-control ARL_1 values.
- Step 4: For the mean shift vector of interest (τ_1, τ_2) , choose the combination of k and H corresponding to the minimum out-of-control ARL_1 value as the optimal design parameters.

(Please insert Table 1 here)

3.2 Steady-state case

Compared with the zero-state case, the steady-state case seems more informative and realistic. Szarka III and Woodall²⁵ summarized two different shift models in the steady-state case, one is the fixed-shift model, and the other one is the random-shift model. The fixed-shift model is to observe a certain number, say q , in-control observations before a shift occurs, and the period of running q in-control observations before a shift occurs is called as the “warm-up period”. This model has been used by many researchers, see for instance Dickinson et al.³⁰ and Xu and Jeske³¹. Different from the fixed-shift model, the random-shift model is based on the assumption that a shift occurs at any time, instead of an immediate shift after a warm-up period. For more details about the random-shift model the reader can refer to Wu and Spedding³².

In this paper, we investigate the steady-state ARL performance using the fixed-shift model. Except for the warm-up period, the Monte-Carlo type procedure for the steady-state ARL performance is similar to the zero-state case one, which can be described as follows:

- Step 1: Specify the design parameters k and H , the scale parameters θ_1 and θ_2 , the number q of the in-control observations in the warm-up period and the dependence parameter δ of the GBE model.
- Step 2: Generate q in-control random vectors $\mathbf{X}_t = (X_{1,t}, X_{2,t})^\top$ of the $GBE(\theta_1, \theta_2, \delta)$ model at time $t = 1, 2, \dots, q$, using (10), (11) and (12).
- Step 3: Run the procedure in the in-control state for these q random vectors before a shift in the scale parameters (θ_1, θ_2) occurs (say, run a warm-up period). If a signal is given during the warm-up period, we discard these q in-control random vectors, and the control flow goes back to Step (2) to generate a new in-control random vector set. Otherwise, the control flow proceeds to the next step.
- Step 4: Generate out-of-control random vectors $\mathbf{X}_t = (X_{1,t}, X_{2,t})^\top$ of the $GBE(\theta'_1, \theta'_2, \delta)$ model at time $t = q + 1, q + 2, \dots$, using (10), (11) and (12).
- Step 5: Calculate the steady-state MCUSUM statistic \mathbf{S}_t , and the corresponding statistic Q_t at time $t = q + 1, q + 2, \dots$, using (7), (8) and (9).

Step 6: If the statistic $Q_t > H$, the process is deemed to be out-of-control, and the corresponding steady-state RL, which equals to $t - q$, is recorded.

Step 7: Repeat Steps (2)-(6) to obtain 5×10^4 RL values, and the steady-state ARL value can be obtained by averaging these ones.

In the steady-state case, the procedure for determining the optimal design parameters k and H of the proposed MCUSUM GBE chart is similar to the one in the zero-state case, except that the number q of the in-control observations of the warm-up period has to be fixed first. Table 2 shows the combinations of design parameters k and H leading to the desired $ARL_0 \in \{100, 200, 370\}$ when the dependency parameter $\delta \in \{0.2, 0.5, 0.7, 0.9\}$ and the number of the in-control observations of the warm-up period $q = 50$.

(Please insert Table 2 here)

4 Comparison study

The ARL performances of the proposed MCUSUM GBE, MEWMA and paired individual CUSUM charts are compared in this section. The MEWMA chart proposed in Xie et al.²² for monitoring the GBE model is first introduced and then it is compared with the proposed MCUSUM GBE chart in both zero- and steady-state cases.

4.1 The MEWMA chart

The MEWMA chart was firstly introduced in Lowry et al.¹². As the natural extension of the univariate EWMA chart, the MEWMA chart is also sensitive to detect small or moderate shifts in multivariate processes. In addition, it has also been shown that the MEWMA control chart with a small smoothing parameter is fairly robust to the GBE data (see Xie et al.²²).

In the case of GBE data, the MEWMA statistic \mathbf{Y}_t is defined as,

$$\mathbf{Y}_t = \mathbf{R}(\mathbf{X}_t - \boldsymbol{\mu}_0) + (\mathbf{I} - \mathbf{R})\mathbf{Y}_{t-1}, \quad (13)$$

where the process initial statistic $\mathbf{Y}_0 = \mathbf{0}$, $\mathbf{R} = \text{diag}(r_1, r_2)$, $r_j \in (0, 1]$ for $j = 1, 2$, and \mathbf{I} is the $(2, 2)$ identity matrix. The statistic $Q'_t{}^2$ of the MEWMA control chart is,

$$Q'_t{}^2 = \mathbf{Y}_t^T \boldsymbol{\Sigma}_{\mathbf{Y}_t}^{-1} \mathbf{Y}_t, \quad (14)$$

where $\boldsymbol{\Sigma}_{\mathbf{Y}_t}$ is the in-control variance-covariance matrix of \mathbf{Y}_t . When $r_1 = r_2 = r$, the MEWMA statistic can simply be re-stated as,

$$\mathbf{Y}_t = r(\mathbf{X}_t - \boldsymbol{\mu}_0) + (1 - r)\mathbf{Y}_{t-1}. \quad (15)$$

In addition, the asymptotic in-control variance-covariance matrix $\boldsymbol{\Sigma}_{\mathbf{Y}_t}$ is,

$$\boldsymbol{\Sigma}_{\mathbf{Y}_t} = \left(\frac{r}{2 - r} \right) \boldsymbol{\Sigma}, \quad (16)$$

where $\boldsymbol{\Sigma}$ is the in-control variance-covariance matrix of the random vector \mathbf{X}_t . Hence, the statistic $Q'_t{}^2$ can be re-state as,

$$Q'_t{}^2 = \frac{2 - r}{r} \mathbf{Y}_t^T \boldsymbol{\Sigma}^{-1} \mathbf{Y}_t. \quad (17)$$

If the statistic $Q_t^2 > H'$, the chart generates an out-of-control signal, where $H' > 0$ is the upper control limit of the MEWMA chart. Moreover, when $r = 1$, the MEWMA chart reduces to the Hotelling T^2 chart, which is known to be powerful in detecting large shifts in multivariate processes.

The MEWMA chart with smoothing parameters $r \in \{0.02, 0.1, 0.5, 1\}$ in Xie et al.²² are compared with the MCUSUM GBE chart proposed in this paper. To provide a fair comparison, both of them are designed to have the same ARL_0 for zero- and steady-state cases.

4.2 The Paired individual CUSUM chart

The paired individual CUSUM chart consists of two univariate CUSUM charts, which are used to monitor the variables X_1 and X_2 , respectively. For the paired individual CUSUM chart, we assume that the variables X_1 and X_2 follow the exponential distribution respectively with the following survival functions,

$$\bar{F}_{X_i}(x_i) = \exp\left(-\frac{x_i}{\theta_i}\right) \quad (i = 1, 2). \quad (18)$$

Without loss of generality, the following scaling of the variables X_1 and X_2 is considered,

$$Z_i = \frac{X_i}{\theta_i} \quad (i = 1, 2). \quad (19)$$

Therefore, the statistics of these two univariate charts can be re-stated as,

$$\begin{cases} C_{1,t}^+ = \max(0, Z_{1,t} - 1 - k + C_{1,t-1}^+), \\ C_{1,t}^- = \max(0, -Z_{1,t} + 1 - k + C_{1,t-1}^-). \end{cases} \quad (20)$$

$$\begin{cases} C_{2,t}^+ = \max(0, Z_{2,t} - 1 - k + C_{2,t-1}^+), \\ C_{2,t}^- = \max(0, -Z_{2,t} + 1 - k + C_{2,t-1}^-). \end{cases} \quad (21)$$

where the initial values are set as $C_{1,0}^+ = C_{1,0}^- = C_{2,0}^+ = C_{2,0}^- = 0$. The paired individual CUSUM chart signals if any one of the statistic, say, $C_{1,t}^+, C_{1,t}^-, C_{2,t}^+, C_{2,t}^-$, exceed the control limits h_1 or h_2 .

In this study, we equally allocate the Type I error α between these two univariate CUSUM charts, i.e., $\alpha_1 = \alpha_2 = \alpha/2$, where α_1 and α_2 are the Type I errors assigned to these two univariate CUSUM charts, respectively. In addition, we use the mean shift vector $(\tau_1, \tau_2) = (1, 1)$ to denote the in-control state. Hence, when the same reference parameter k is set for these two univariate CUSUM charts, the control limits of these ones are equal, say, $h_1 = h_2 = h$.

In the case of GBE data, it can also be proved that, the ARL performance of each univariate CUSUM chart only depends on the ratio of the scale parameter $\tau = \theta'/\theta$, the reference parameter k and the control limit h .

For comparison, we keep the ARL_0 value and the reference parameter k of the paired individual CUSUM chart the same as those in the proposed MCUSUM GBE chart, the value of the control limit h can be obtained using the constraint on the desired ARL_0 . Then for different shifts, the out-of-control ARL_1 values can be calculated.

4.3 Comparisons under different types of shifts

To evaluate the performance of the proposed MCUSUM GBE chart, the control limits H of the chart (using the constraint on the ARL_0 in zero- and steady-state cases) are presented in Tables 1 and 2, respectively, for different values of $ARL_0 \in \{100, 200, 370\}$ and dependency parameter $\delta \in \{0.2, 0.5, 0.7, 0.9\}$ when the reference parameter k ranges from 0.02 to 3.

In addition, when the process is out-of-control, three different types of shift are considered to evaluate the out-of-control ARL_1 performance of the proposed MCUSUM GBE, MEWMA and paired individual CUSUM charts:

1. a downward shift,
2. an upward shift,
3. and a hybrid shift.

These three types of shift are defined and investigated in the following subsections.

4.3.1 Downward shift detection

A downward shift occurs in the process if

- either X_1 shifts downward but X_2 does not shift. This corresponds to the case $(\tau_1 < 1, \tau_2 = 1)$,
- or X_1 does not shift but X_2 shifts downward. This corresponds to the case $(\tau_1 = 1, \tau_2 < 1)$,
- or both X_1 and X_2 shift downward. This corresponds to the case $(\tau_1 < 1, \tau_2 < 1)$.

The first two cases are classified as “single downward shifts” while the third one is classified as “double downward shift”. Due to the scaling/standardization, it is noted that both case $(\tau_1 < 1, \tau_2 = 1)$ and case $(\tau_1 = 1, \tau_2 < 1)$ have the same ARL values, thus we only investigated the ARL performance of the case $(\tau_1 < 1, \tau_2 = 1)$ for the single downward shift detection.

The downward shift detection of the GBE model is very important when the events we are interested in are negative ones, such as nonconformities and defects in quality control applications. The downward shift in these cases represents the fact that the time between two nonconformities or defects becomes shorter than before. That is to say, the ratio of nonconformities or defects increases, and the quality of the product deteriorates.

Different combinations of k and H that produce the desired ARL_0 value are considered to evaluate the out-of-control properties of the proposed MCUSUM GBE chart, see Tables 1 and 2. Without loss of generality, assuming $\theta_1 = 1$, $\theta_2 = 1$, $\delta = 0.5$ and $ARL_0 = 200$, then both zero- and steady-state ARLs of the chart for different downward shifts are presented in Tables 3 and 4, respectively. For example, when $(\tau_1, \tau_2) = (0.2, 1)$, the zero-state ARL_1 values equal to 14.87 and 15.23 for $k = 0.1$ and 0.6, respectively (see Table 3), and the corresponding steady-state ARL_1 values equal to 14.38 and 14.86, respectively (see Table 4).

As a matter of comparison, when $ARL_0 = 200$, the properties of the MEWMA chart (proposed in Xie et al.²² with different combinations of the smoothing parameter $r \in \{0.02, 0.1, 0.5, 1\}$ and the corresponding control limit H') and the paired individual CUSUM chart (with different combinations of the reference parameter k and the corresponding control limit h) are also presented in Tables 3

and 4. For example, when $(\tau_1, \tau_2) = (0.2, 1)$, the zero-state ARL_1' value of the MEWMA chart equals to 13.40 for $r = 0.1$ (see Table 3), and the corresponding steady-state ARL_1' value equals to 12.97 (see Table 4). Meanwhile, for the paired individual CUSUM chart, when $(\tau_1, \tau_2) = (0.2, 1)$, the zero-state ARL_1^* values equal to 18.82 and 27.56 for $k = 0.1$ and 0.6, respectively (see Table 3), and the corresponding steady-state ARL_1^* values equal to 15.55 and 27.03, respectively (see Table 4).

The steady-state properties of these charts in Table 4 have been obtained by simulations with $q = 50$ in-control observations during the warm-up period. For the predetermined downward shift vectors (τ_1, τ_2) , the minimum out-of-control ARL_1 values of these charts (say, ARL_{\min} , ARL'_{\min} and ARL^*_{\min}) are bolded in these tables. From Tables 3 and 4, several conclusions can be drawn as follows:

(Please insert Tables 3 and 4 here)

- (1) For the downward shift domain studied in this paper, the optimal reference parameters k_{opt} of the MCUSUM GBE chart are all smaller than 0.4. For example, when (τ_1, τ_2) equal to $(0.8, 1)$ and $(0.1, 1)$, the optimal reference parameters k_{opt} are 0.1 and 0.3 in both zero- and steady-state cases (see Tables 3 and 4). In addition, for a downward shift detection, it is indicated that the proposed MCUSUM GBE chart with a small reference parameter (say, $k \in [0.1, 0.4]$) is more effective than the chart with a large reference parameter. For example, when $(\tau_1, \tau_2) = (0.1, 0.1)$, the zero-state ARL_1 values equal to 12.47 and 19.27 for $k = 0.2$ and 0.7, respectively (see Table 3), and the corresponding steady-state ARL_1 values equal to 11.68 and 19.11, respectively (see Table 4).
- (2) The proposed MCUSUM GBE chart seems more effective than the MEWMA chart to detect a downward shift. For the downward shift domain, almost every ARL_{\min} of the proposed MCUSUM GBE chart are smaller than ones ARL'_{\min} of the MEWMA chart. For example, when $(\tau_1, \tau_2) = (0.8, 1)$, the zero-state ARL_{\min} and ARL'_{\min} are 66.33 and 68.30, respectively (see Table 3). Meanwhile, the corresponding steady-state ARL_{\min} and ARL'_{\min} are 63.07 and 65.08, respectively (see Table 4).
- (3) With the same reference parameter k , the proposed MCUSUM GBE chart is more effective than the paired individual CUSUM chart for detecting a *single* downward shift. For example, when $(\tau_1, \tau_2) = (0.5, 1)$ and $k = 0.2$, the zero-state ARL_1 and ARL_1^* values are 22.08 and 29.73, respectively (see Table 3). Meanwhile, the corresponding steady-state ARL_1 and ARL_1^* values are 20.70 and 25.51, respectively (see Table 4).
- (4) In the steady-state case, the paired individual CUSUM chart seems to be a bit more effective than the proposed MCUSUM GBE chart to detect a *double* downward shift. For example, when $(\tau_1, \tau_2) = (0.5, 0.5)$, the steady-state ARL_{\min} and ARL^*_{\min} values are 24.33 and 23.40, respectively (see Table 4).
- (5) Let η' and η^* be the relative differences between ARL_{\min} , ARL'_{\min} and ARL^*_{\min} , respectively, i.e.,

$$\eta' = \frac{ARL_{\min} - AR L'_{\min}}{AR L'_{\min}} \times 100\%, \quad (22)$$

$$\eta^* = \frac{ARL_{\min} - AR L^*_{\min}}{AR L^*_{\min}} \times 100\%. \quad (23)$$

Furthermore, let $\bar{\eta}'$ and $\bar{\eta}^*$ be the average of the η' and η^* values obtained for all the shifts (τ_1, τ_2) considered in Tables 3 and 4, respectively. As it can be seen, $\bar{\eta}'$ of the chart for the zero- and steady-state cases are -5.60% and -5.88% , respectively, and $\bar{\eta}^*$ of the chart for the zero- and steady-state cases are -15.29% and -6.57% , respectively. This fact indicates that the proposed MCUSUM GBE chart outperforms the MEWMA and paired individual CUSUM charts for the whole downward shift domain, in average.

4.3.2 Upward shift detection

An upward shift occurs in the process if

- either X_1 shifts upward but X_2 does not shift. This corresponds to the case $(\tau_1 > 1, \tau_2 = 1)$,
- or X_1 does not shift but X_2 shifts upward. This corresponds to the case $(\tau_1 = 1, \tau_2 > 1)$,
- or both X_1 and X_2 shift upward. This corresponds to the case $(\tau_1 > 1, \tau_2 > 1)$.

Similar to the downward shift detection, the first two cases are classified as “single upward shifts” and the third one is classified as “double upward shift”. In addition, for the similar reason, we also only investigated the ARL performance of the case $(\tau_1 > 1, \tau_2 = 1)$ for the single upward shift detection.

The upward shift detection is critical when the events we are interested in are positive ones, such as purchase orders of a production. Similar to the settings in the downward shift case, let us assume $\theta_1 = 1, \theta_2 = 1, \delta = 0.5$ and $ARL_0 = 200$. For different upward shifts, zero- and steady-state ARLs of the chart are shown in Tables 5 and 6, respectively. For example, when $(\tau_1, \tau_2) = (2, 1)$, the zero-state ARL_1 values equal to 12.89 and 10.13 for $k = 0.1$ and 0.6, respectively (see Table 5), and the corresponding steady-state ARL_1 values equal to 12.70 and 9.85, respectively (see Table 6).

To provide a comparison, when $ARL_0 = 200$, the properties of the MEWMA chart (with different combinations of the smoothing parameter $r \in \{0.02, 0.1, 0.5, 1\}$ and the corresponding control limit H') and the paired individual CUSUM chart (with different combinations of the reference parameter k and the corresponding control limit h) are also presented in Tables 5 and 6. For example, when $(\tau_1, \tau_2) = (2, 1)$, the zero-state ARL_1' value of the MEWMA chart equals to 9.65 for $r = 0.1$ (see Table 5), and the corresponding steady-state ARL_1' value equals to 9.55 (see Table 6). Meanwhile, for the paired individual CUSUM chart, when $(\tau_1, \tau_2) = (2, 1)$, the zero-state ARL_1^* values equal to 15.76 and 12.18 for $k = 0.1$ and 0.6, respectively (see Table 5), and the corresponding steady-state ARL_1^* values equal to 13.74 and 11.89, respectively (see Table 6).

Moreover, as for the upward shift case, the steady-state properties of these charts in Table 6 have been obtained by simulations with $q = 50$ in-control observations during the warm-up period, and the minimum out-of-control ARL_1 of these charts (say, ARL_{\min} , ARL'_{\min} and ARL^*_{\min}) are bolded in these tables. From Tables 5 and 6, several conclusions can be drawn as follows:

(Please insert Tables 5 and 6 here)

- (1) For the upward shift domain studied in this paper, the optimal reference parameters k_{opt} of the MCUSUM GBE chart are all larger than or equal to 0.3. For example, when (τ_1, τ_2) equal to $(2, 1)$ and $(5, 1)$, the optimal reference parameters k_{opt} in the zero-state case are 0.4 and 0.8, respectively (see Table 5). Meanwhile, the corresponding optimal reference parameters k_{opt} in the steady-state case are 0.4 and 1, respectively (see Table 6).

- (2) Almost every ARL_{\min} of the proposed MCUSUM GBE chart are smaller than the corresponding ARL'_{\min} of the MEWMA chart in the steady-state case. This indicates that the proposed MCUSUM GBE chart outperforms the MEWMA chart for detecting an upward shift in the steady-state case. For example, when $(\tau_1, \tau_2) = (1.5, 1)$, the steady-state ARL_{\min} and ARL'_{\min} are 20.86 and 22.17, respectively (see Table 6).
- (3) With the same reference parameter k , the proposed MCUSUM GBE chart is more effective than the paired individual CUSUM chart for detecting a *single* upward shift. For example, when $(\tau_1, \tau_2) = (2, 1)$ and $k = 0.2$, the zero-state ARL_1 and ARL_1^* values are 10.85 and 12.85, respectively (see Table 5). Meanwhile, the corresponding steady-state ARL_1 and ARL_1^* values are 10.52 and 11.59, respectively (see Table 6). However, for the *double* upward shift domain, most ARL_1 values of the proposed MCUSUM GBE chart are larger than the corresponding ARL_1^* values of the paired individual CUSUM chart. For example, when $(\tau_1, \tau_2) = (1.5, 1.5)$ and $k = 0.2$, the zero-state ARL_1 and ARL_1^* values are 21.25 and 20.68, respectively (see Table 5). Meanwhile, the corresponding steady-state ARL_1 and ARL_1^* values are 20.58 and 18.62, respectively (see Table 6).
- (4) For the proposed MCUSUM GBE chart and the MEWMA chart, the $\bar{\eta}'$ of the chart for the zero- and steady-state cases are -0.12% and -1.52% , respectively. Meanwhile, for the proposed MCUSUM GBE chart and the paired individual CUSUM chart, the $\bar{\eta}^*$ of the chart for the zero- and steady-state cases are -6.03% and -4.60% , respectively. That is to say, the proposed MCUSUM GBE chart also outperforms, in average, the MEWMA and paired individual CUSUM charts for the whole upward shift domain.

4.3.3 Hybrid shift detection

A hybrid shift occurs in the process if

- either X_1 shifts downward while X_2 shifts upward. This corresponds to the case $(\tau_1 < 1, \tau_2 > 1)$,
- or X_1 shifts upward while X_2 shifts downward. This corresponds to the case $(\tau_1 > 1, \tau_2 < 1)$.

The same settings as in the downward shift case are also specified for the hybrid shift case, say, $\theta_1 = 1$, $\theta_2 = 1$, $\delta = 0.5$, $ARL_0 = 200$. For different hybrid shifts, both zero- and steady-state ARLs of the chart are investigated, and the results are presented in Tables 7 and 8, respectively. For example, when $(\tau_1, \tau_2) = (0.5, 2)$, the zero-state ARL_1 values equal to 9.42 and 7.22 for $k = 0.1$ and 0.6, respectively (see Table 7), and the corresponding steady-state ARL_1 equal to 9.31 and 7.01, respectively (see Table 8).

For comparison, when $ARL_0 = 200$, the properties of the MEWMA chart (with different combinations of the smoothing parameter $r \in \{0.02, 0.1, 0.5, 1\}$ and the corresponding control limit H') and the paired individual CUSUM chart (with different combinations of the reference parameter k and the corresponding control limit h) are also presented in Tables 7 and 8. For example, when $(\tau_1, \tau_2) = (0.5, 2)$, the zero-state ARL'_1 value of the MEWMA chart equals to 6.92 for $r = 0.1$ (see Table 7), and the corresponding steady-state ARL'_1 value equals to 6.80 (see Table 8). Meanwhile, for the paired individual CUSUM chart, when $(\tau_1, \tau_2) = (0.5, 2)$, the zero-state ARL_1^* values equal to 14.99 and 12.25 for $k = 0.1$ and 0.6, respectively (see Table 7), and the corresponding steady-state ARL_1^* values equal to 12.47 and 11.93, respectively (see Table 8).

From Tables 7 and 8, several conclusions can be made as follows,

(Please insert Tables 7 and 8 here)

- (1) For the hybrid shift domain studied in this paper, the optimal reference parameters k_{opt} of the MCUSUM GBE chart are all larger than or equal to 0.3. For example, when (τ_1, τ_2) equal to $(0.8, 1.5)$ and $(0.5, 2)$, the optimal reference parameters k_{opt} are 0.3 and 0.4 in both zero- and steady-state cases (see Table 7 and 8).
- (2) Almost every ARL_{\min} of the proposed MCUSUM GBE chart are smaller than the corresponding ARL'_{\min} of the MEWMA chart in the steady-state case. This indicates that the proposed MCUSUM GBE chart is superior to the MEWMA chart for detecting a hybrid shift in the steady-state case. For example, when $(\tau_1, \tau_2) = (0.8, 1.5)$, the steady-state ARL_{\min} and ARL'_{\min} are 16.05 and 17.42, respectively (see Table 8).
- (3) With the same reference parameter k , the ARL_1 value of the proposed MCUSUM GBE chart is significantly smaller than the ARL_1^* value of the paired individual CUSUM chart. For example, when $(\tau_1, \tau_2) = (0.8, 1.5)$ and $k = 0.4$, the zero-state ARL_1 and ARL_1^* values are 17.27 and 28.29, respectively (see Table 7). Meanwhile, the corresponding steady-state ARL_1 and ARL_1^* values are 16.71 and 27.24, respectively (see Table 8). It is indicated that the proposed MCUSUM GBE chart is more effective than the paired individual CUSUM chart in a hybrid shift detection.
- (4) For the proposed MCUSUM GBE chart and the MEWMA chart, the $\bar{\eta}'$ of the chart for the zero- and steady-state cases are -1.11% and -2.55% , respectively. Meanwhile, for the proposed MCUSUM GBE chart and the paired individual CUSUM chart, the $\bar{\eta}^*$ of the chart for the zero- and steady-state cases are -26.04% and -23.47% , respectively. That is to say, the proposed MCUSUM GBE chart also outperforms the MEWMA and paired individual CUSUM charts for the whole hybrid shift domain, in average.

5 An illustrative example of the MCUSUM GBE chart

A patient relief time example is given to illustrate the monitoring procedure of the proposed MCUSUM GBE chart. In this example, each of the 10 patients under consideration was given a standard treatment and a new treatment for headache. The corresponding length of relief time (in minutes) from headache are denoted as X_1 and X_2 , respectively. All the values of (X_1, X_2) can be found in Gross and Lam³³ as $(8.40, 6.90)$, $(7.70, 6.80)$, $(10.10, 10.30)$, $(9.60, 9.40)$, $(9.30, 8.00)$, $(9.10, 8.80)$, $(9.00, 6.10)$, $(7.70, 7.40)$, $(8.10, 8.00)$, $(5.30, 5.10)$. For the plausibility of exponential marginal distributions, Gross and Lam³³ transformed these 10 couples by subtracting a threshold value of 5.0 from each data point (see No.1-10 in Columns 2 and 3 in Table 9).

As an illustrative example, using these 10 transformed couples as the in-control data, the average transformed relief time $\hat{\mu}$ can be estimated by using the following equation,

$$\hat{\mu} = \bar{\mathbf{X}} = \frac{1}{n} \sum_{t=1}^n \mathbf{X}_t, \quad (24)$$

Meanwhile, the dependency parameter δ can be estimated using the estimator proposed in Lu and Bhattacharyya²⁸,

$$\hat{\delta} = -\log_2 \left(\frac{1}{n} \sum_{t=1}^n \min \left(\frac{X_{1,t}}{\bar{X}_1}, \frac{X_{2,t}}{\bar{X}_2} \right) \right), \quad (25)$$

where $n = 10$. Then the estimated scale parameters are $\hat{\theta}_1 = 3.43$ and $\hat{\theta}_2 = 2.68$, the estimated dependency parameter is $\hat{\delta} = 0.2072$.

Following Xie et al.²², it is assumed that if a new effective medicine is used in combination with each of these two treatments, then the corresponding average transformed relief time of these two treatments can be shortened to 20% and 50%, say, $(\tau_1 = 0.2, \tau_2 = 0.5)$. Based on this assumption, we generate the next 20 transformed couples by setting the scale parameters $(\theta'_1, \theta'_2) = (0.2\hat{\theta}_1, 0.5\hat{\theta}_2) = (0.69, 1.34)$, and keeping the dependency parameter $\delta' = \hat{\delta} = 0.2072$. All these 30 couples are shown in Table 9.

The combinations of the reference parameter k and the control limit H are determined to achieve the desired in-control $ARL_0 = 200$. For example, when the reference parameter $k = 0.1$ and the dependency parameter $\delta = 0.2072$, it is easy to obtain the control limit $H = 12.89$. The MCUSUM statistic \mathbf{S}_t and the corresponding statistic Q_t are also shown in Table 9 (see Columns 5, 6 and 7 in Table 9). In addition, the monitoring procedure of the proposed MCUSUM GBE chart for these 30 transformed couples is shown in Figure 1. As we can see, the proposed MCUSUM GBE chart generates an out-of-control signal at the 19th observation, which is the 9th observation after the shift has occurred.

(Please insert Table 9 here)

(Please insert Figure 1 here)

6 Conclusion

In order to monitor Gumbel's Bivariate Exponential data, a MCUSUM type chart is proposed. Both zero- and steady-state ARL properties of the proposed MCUSUM GBE chart have been investigated using Monte Carlo simulations. In addition, an illustrative example is given to demonstrate the monitoring procedure of the proposed MCUSUM GBE chart. Comparisons among the proposed MCUSUM GBE, MEWMA and paired individual CUSUM charts have been conducted. With the effect of the correlation between variables, the paired individual CUSUM chart can detect the double downward and double upward shifts faster than the proposed MCUSUM GBE chart in some circumstances. However, if we consider the whole shift domain in both zero- and steady-state cases, it is obvious that the proposed MCUSUM GBE chart performs better than the other two charts, especially in the steady-state case.

The current work could be extended to investigate other multivariate distributions, like, for example, the bivariate gamma or the bivariate Weibull distributions. In addition, for Gumbel's Bivariate Exponential data, it would be interesting to develop new improved multivariate control charts for monitoring the process dispersion or both the process mean and dispersion simultaneously.

References

- [1] DC Montgomery. *Statistical quality control*. Wiley New York, 2009.
- [2] M Xie, TN Goh, and V Kuralmani. *Statistical models and control charts for high-quality processes*. Springer Science & Business Media, 2012.
- [3] LY Chan, M Xie, and TN Goh. Cumulative quantity control charts for monitoring production processes. *International Journal of Production Research*, 38(2):397–408, 2000.
- [4] JY Liu, M Xie, TN Goh, and PR Sharma. A comparative study of exponential time between events charts. *Quality Technology & Quantitative Management*, 3(3):347–359, 2006.
- [5] JY Liu, M Xie, TN Goh, and LY Chan. A study of EWMA chart with transformed exponential data. *International Journal of Production Research*, 45(3):743–763, 2007.
- [6] CW Zhang, M Xie, JY Liu, and TN Goh. A control chart for the Gamma distribution as a model of time between events. *International Journal of Production Research*, 45(23):5649–5666, 2007.
- [7] L Zhang and G Chen. EWMA charts for monitoring the mean of censored Weibull lifetimes. *Journal of Quality Technology*, 36(3):321–328, 2004.
- [8] D Rahali, P Castagliola, H Taleb, and MBC Khoo. Evaluation of shewhart time-between-events-and-amplitude control charts for several distributions. *Quality Engineering*, 31(2):240–254, 2019.
- [9] FK Wang, B Bizuneh, and TH Abebe. A comparison study of control charts for Weibull distributed time between events. *Quality and Reliability Engineering International*, 33(8):2747–2759, 2017.
- [10] RB Crosier. Multivariate generalizations of cumulative sum quality-control schemes. *Technometrics*, 30(3):291–303, 1988.
- [11] JJ Pignatiello Jr and GC Runger. Comparisons of multivariate CUSUM charts. *Journal of quality technology*, 22(3):173–186, 1990.
- [12] CA Lowry, WH Woodall, CW Champ, and SE Rigdon. A multivariate exponentially weighted moving average control chart. *Technometrics*, 34(1):46–53, 1992.
- [13] C Zou and F Tsung. A multivariate sign EWMA control chart. *Technometrics*, 53(1):84–97, 2011.
- [14] AA Tang, J Sun, XL Hu, and P Castagliola. A new nonparametric adaptive EWMA control chart with exact run length properties. *Computers & Industrial Engineering*, 130:404–419, 2019.
- [15] M Zhou, Q Zhou, and W Geng. A new nonparametric control chart for monitoring variability. *Quality and Reliability Engineering International*, 32(7):2471–2479, 2016.
- [16] J Yue and L Liu. Multivariate nonparametric control chart with variable sampling interval. *Applied Mathematical Modelling*, 52:603–612, 2017.
- [17] RG Kittlitz Jr. Transforming the exponential for SPC applications. *Journal of Quality Technology*, 31(3):301–308, 1999.

- [18] YS Chang and DS Bai. A multivariate T^2 control chart for skewed populations using weighted standard deviations. *Quality and Reliability Engineering International*, 20(1):31–46, 2004.
- [19] YS Chang. Multivariate CUSUM and EWMA control charts for skewed populations using weighted standard deviations. *Communications in Statistics–Simulation and Computation*, 36(4):921–936, 2007.
- [20] ZG Stoumbos and JH Sullivan. Robustness to non-normality of the multivariate EWMA control chart. *Journal of Quality Technology*, 34(3):260–276, 2002.
- [21] MC Testik, GC Runger, and CM Borrór. Robustness properties of multivariate EWMA control charts. *Quality and Reliability Engineering International*, 19(1):31–38, 2003.
- [22] Y Xie, M Xie, and TN Goh. Two MEWMA charts for Gumbel’s bivariate exponential distribution. *Journal of Quality Technology*, 43(1):50–65, 2011.
- [23] EJ Gumbel. Bivariate exponential distributions. *Journal of the American Statistical Association*, 55(292):698–707, 1960.
- [24] MBC Khoo. A moving average control chart for monitoring the fraction non-conforming. *Quality and Reliability Engineering International*, 20(6):617–635, 2004.
- [25] JL Szarka III and WH Woodall. On the equivalence of the Bernoulli and geometric CUSUM charts. *Journal of Quality Technology*, 44(1):54–62, 2012.
- [26] S Knoth. The steady-state behavior of multivariate exponentially weighted moving average control charts. *Sequential Analysis*, 37(4):511–529, 2018.
- [27] CA Lowry and DC Montgomery. A review of multivariate control charts. *IIE transactions*, 27(6):800–810, 1995.
- [28] JC Lu and GK Bhattacharyya. Inference procedures for bivariate exponential model of Gumbel. *Statistics & probability letters*, 12(1):37–50, 1991.
- [29] RB Crosier. A new two-sided cumulative sum quality control scheme. *Technometrics*, 28(3):187–194, 1986.
- [30] RM Dickinson, DAO Roberts, AR Driscoll, WH Woodall, and GG Vining. CUSUM charts for monitoring the characteristic life of censored Weibull lifetimes. *Journal of Quality Technology*, 46(4):340–358, 2014.
- [31] S Xu and DR Jeske. Weighted EWMA charts for monitoring type I censored Weibull lifetimes. *Journal of Quality Technology*, 50(2):220–230, 2018.
- [32] Z Wu and TA Spedding. Evaluation of ATS for CRL control chart. *Process Control and Quality*, 11(3):183–191, 1999.
- [33] AJ Gross and CF Lam. Paired observations from a survival distribution. *Biometrics*, 37(3):505–511, 1981.

Table 1: The values of control limit H of the proposed MCUSUM GBE chart in the zero-state case for $ARL_0 \in \{100, 200, 370\}$, $\delta \in \{0.2, 0.5, 0.7, 0.9\}$ and $k \in \{0.02, 0.05, 0.07, 0.1, 0.2, 0.3, 0.4, 0.5, 0.6, 0.7, 0.8, 0.9, 1, 3\}$

ARL ₀	δ	k													
		0.02	0.05	0.07	0.1	0.2	0.3	0.4	0.5	0.6	0.7	0.8	0.9	1	3
100	0.2	12.44	11.30	10.65	9.80	7.75	6.60	5.99	5.61	5.33	5.09	4.85	4.67	4.49	2.02
	0.5	12.50	11.41	10.73	9.88	7.78	6.55	5.84	5.41	5.09	4.82	4.61	4.41	4.19	1.69
	0.7	12.55	11.43	10.77	9.89	7.79	6.50	5.75	5.31	4.96	4.70	4.45	4.26	4.07	1.55
	0.9	12.57	11.43	10.77	9.91	7.78	6.51	5.72	5.24	4.88	4.62	4.38	4.17	3.97	1.45
200	0.2	17.52	15.47	14.29	12.85	9.79	8.28	7.53	7.01	6.62	6.30	6.05	5.78	5.56	2.91
	0.5	17.59	15.52	14.34	12.90	9.78	8.14	7.24	6.68	6.27	5.93	5.63	5.38	5.15	2.46
	0.7	17.58	15.47	14.34	12.91	9.77	8.07	7.13	6.53	6.10	5.75	5.44	5.19	4.96	2.27
	0.9	17.59	15.51	14.37	12.91	9.75	8.04	7.06	6.44	6.01	5.64	5.33	5.10	4.85	2.16
370	0.2	23.31	19.88	18.09	15.99	11.77	9.90	8.94	8.30	7.80	7.40	7.09	6.80	6.54	3.75
	0.5	23.48	19.95	18.18	16.01	11.70	9.63	8.56	7.83	7.31	6.88	6.56	6.26	6.01	3.16
	0.7	23.48	19.95	18.18	16.00	11.64	9.53	8.40	7.66	7.10	6.69	6.32	6.04	5.78	2.92
	0.9	23.47	20.03	18.18	16.00	11.61	9.48	8.31	7.54	6.98	6.57	6.20	5.90	5.64	2.78

Table 2: The values of control limit H of the proposed MCUSUM GBE chart in the steady-state case, for $ARL_0 \in \{100, 200, 370\}$, $\delta \in \{0.2, 0.5, 0.7, 0.9\}$ and $k \in \{0.02, 0.05, 0.07, 0.1, 0.2, 0.3, 0.4, 0.5, 0.6, 0.7, 0.8, 0.9, 1, 3\}$

ARL ₀	δ	k													
		0.02	0.05	0.07	0.1	0.2	0.3	0.4	0.5	0.6	0.7	0.8	0.9	1	3
100	0.2	14.23	12.60	11.65	10.49	7.99	6.69	6.03	5.64	5.35	5.11	4.85	4.67	4.48	1.99
	0.5	14.31	12.65	11.75	10.60	8.05	6.67	5.89	5.47	5.13	4.87	4.62	4.41	4.23	1.68
	0.7	14.39	12.69	11.81	10.61	8.05	6.66	5.84	5.35	5.00	4.72	4.48	4.27	4.08	1.55
	0.9	14.41	12.70	11.82	10.63	8.07	6.66	5.80	5.28	4.90	4.64	4.41	4.18	3.97	1.46
200	0.2	19.27	16.69	15.28	13.53	10.00	8.36	7.56	7.03	6.63	6.32	6.03	5.79	5.57	2.90
	0.5	19.33	16.72	15.28	13.56	9.99	8.23	7.29	6.71	6.28	5.94	5.64	5.38	5.16	2.46
	0.7	19.30	16.69	15.32	13.53	9.98	8.15	7.18	6.55	6.11	5.76	5.47	5.20	4.98	2.28
	0.9	19.29	16.73	15.33	13.62	9.97	8.13	7.10	6.49	6.02	5.65	5.35	5.09	4.86	2.16
370	0.2	24.81	20.85	18.82	16.45	11.90	9.95	8.97	8.29	7.81	7.42	7.10	6.79	6.53	3.75
	0.5	24.82	20.85	18.84	16.47	11.84	9.71	8.59	7.86	7.30	6.91	6.58	6.28	6.01	3.15
	0.7	24.82	20.86	18.87	16.49	11.81	9.62	8.43	7.66	7.13	6.69	6.34	6.05	5.78	2.91
	0.9	24.85	20.88	18.92	16.51	11.80	9.55	8.32	7.57	6.99	6.57	6.21	5.90	5.63	2.79

Table 3: Zero-state ARLs of different charts for the downward shift domain when $\delta = 0.5$ and $ARL_0 = 200$

		MCUSUM GBE / Paired individual CUSUM																	MEWMA				
k		0.02	0.05	0.07	0.1	0.2	0.3	0.4	0.5	0.6	0.7	0.8	0.9	1	3	r	0.02	0.1	0.5	1			
(τ_1, τ_2)	H	17.59	15.52	14.34	12.90	9.78	8.14	7.24	6.68	6.27	5.93	5.63	5.38	5.15	2.46	H'	5.28	10.34	23.60	29.55			
	h	19.45	16.34	14.73	12.83	9.24	7.58	6.69	6.11	5.65	5.30	5.01	4.76	4.53	1.97								
(1, 1)	ARL_0	199.84	200.75	199.55	200.01	199.64	199.96	199.32	199.72	199.88	199.48	199.75	199.96	199.68	199.82	ARL'_0	199.96	200.20	199.31	199.81			
	ARL_0^*	199.89	200.69	200.41	199.60	199.85	199.65	199.54	199.90	199.46	199.18	199.02	200.93	200.78	199.71								
(0.8, 1)	ARL_1	70.32	67.92	66.73	66.33	75.36	105.60	165.97	*	*	*	*	*	*	*	ARL'_1	68.30	183.57	*	*			
	ARL_1^*	94.33	89.27	87.91	88.86	118.31	*	*	*	*	*	*	*	*	*								
(0.5, 1)	ARL_1	29.36	27.08	25.88	24.41	22.08	22.73	26.67	35.59	56.69	94.54	132.78	160.88	182.68	*	ARL'_1	22.86	39.44	*	*			
	ARL_1^*	40.79	36.52	34.32	31.93	29.73	34.55	51.59	125.28	*	*	*	*	*	*								
(0.2, 1)	ARL_1	18.62	16.93	15.98	14.87	12.63	11.93	12.22	13.32	15.23	18.43	24.05	34.68	52.38	169.13	ARL'_1	13.56	13.40	104.41	175.43			
	ARL_1^*	25.45	22.29	20.69	18.82	15.84	15.52	16.96	20.38	27.56	48.40	*	*	*	*								
(0.1, 1)	ARL_1	16.60	15.07	14.22	13.18	11.05	10.31	10.37	10.97	12.14	13.88	16.65	21.34	29.48	141.14	ARL'_1	11.98	10.88	80.74	149.48			
	ARL_1^*	22.60	19.72	18.25	16.52	13.65	13.05	13.74	15.55	18.92	26.13	47.15	*	*	*								
(0.8, 0.8)	ARL_1	78.24	77.12	76.65	77.65	100.43	195.52	*	*	*	*	*	*	*	*	ARL'_1	82.77	*	*	*			
	ARL_1^*	87.47	82.59	81.79	82.50	115.55	*	*	*	*	*	*	*	*	*								
(0.5, 0.5)	ARL_1	32.59	30.32	29.12	27.78	26.23	28.83	37.83	66.15	*	*	*	*	*	*	ARL'_1	26.18	112.74	*	*			
	ARL_1^*	38.64	34.44	32.28	30.01	27.79	32.16	47.94	131.53	*	*	*	*	*	*								
(0.2, 0.2)	ARL_1	20.42	18.70	17.72	16.56	14.40	13.97	14.84	17.00	20.97	29.18	52.52	*	*	*	ARL'_1	15.14	16.55	*	*			
	ARL_1^*	24.99	21.86	20.26	18.42	15.47	15.16	16.56	19.87	26.88	47.72	*	*	*	*								
(0.1, 0.1)	ARL_1	18.17	16.56	15.66	14.58	12.47	11.88	12.26	13.45	15.57	19.27	26.55	46.69	*	*	ARL'_1	13.26	12.82	*	*			
	ARL_1^*	22.40	19.54	18.08	16.35	13.50	12.94	13.63	15.44	18.85	26.13	48.06	*	*	*								

The asterisk (*) represents the ARL value larger than 200.

Table 4: Steady-state ARLs of different charts for the downward shift domain when $\delta = 0.5$ and $ARL_0 = 200$

		MCUSUM GBE / Paired individual CUSUM																	MEWMA				
k		0.02	0.05	0.07	0.1	0.2	0.3	0.4	0.5	0.6	0.7	0.8	0.9	1	3	r	0.02	0.1	0.5	1			
(τ_1, τ_2)	H	19.33	16.72	15.28	13.56	9.99	8.23	7.29	6.71	6.28	5.94	5.64	5.38	5.16	2.46	H'	5.52	10.37	23.62	29.55			
	h	21.43	17.63	15.71	13.52	9.43	7.64	6.74	6.12	5.68	5.31	5.01	4.76	4.53	1.97								
(1, 1)	ARL ₀	199.41	200.41	199.92	199.28	200.52	200.01	200.17	200.31	199.67	200.17	199.39	199.53	200.25	199.41	ARL ₀	200.60	200.23	199.63	200.70			
	ARL ₀ *	200.07	200.36	199.70	199.70	199.23	199.61	200.10	199.88	200.73	199.17	199.64	200.00	200.29	199.72								
(0.8, 1)	ARL ₁	70.94	66.08	63.98	63.07	71.05	102.86	164.87	*	*	*	*	*	*	*	ARL ₁	65.08	184.09	*	*			
	ARL ₁ *	83.35	77.42	76.33	77.25	111.06	*	*	*	*	*	*	*	*	*								
(0.5, 1)	ARL ₁	30.08	26.81	25.22	23.47	20.70	21.52	25.58	34.91	56.04	93.48	132.43	161.28	181.91	*	ARL ₁	21.58	38.90	*	*			
	ARL ₁ *	35.13	30.48	28.40	26.23	25.51	31.32	49.39	123.86	*	*	*	*	*	*								
(0.2, 1)	ARL ₁	19.03	16.86	15.73	14.38	11.92	11.32	11.79	12.95	14.86	18.04	23.68	34.11	52.77	169.83	ARL ₁	12.78	12.97	104.58	176.41			
	ARL ₁ *	22.01	18.67	17.11	15.55	13.46	13.87	15.83	19.52	27.03	47.99	*	*	*	*								
(0.1, 1)	ARL ₁	17.05	15.05	14.03	12.76	10.48	9.81	10.03	10.71	11.87	13.64	16.39	21.15	29.38	142.16	ARL ₁	11.30	10.49	80.99	147.54			
	ARL ₁ *	19.57	16.56	15.14	13.65	11.64	11.66	12.85	14.86	18.51	25.76	46.78	*	*	*								
(0.8, 0.8)	ARL ₁	77.89	73.56	72.67	72.98	94.73	192.37	*	*	*	*	*	*	*	*	ARL ₁	78.37	*	*	*			
	ARL ₁ *	76.63	71.29	69.26	71.05	107.53	*	*	*	*	*	*	*	*	*								
(0.5, 0.5)	ARL ₁	33.10	29.82	28.14	26.27	24.33	27.09	36.48	65.02	*	*	*	*	*	*	ARL ₁	24.42	113.47	*	*			
	ARL ₁ *	32.42	27.80	25.85	23.98	23.40	28.86	46.02	129.76	*	*	*	*	*	*								
(0.2, 0.2)	ARL ₁	20.76	18.48	17.17	15.81	13.46	13.18	14.27	16.53	20.61	28.84	52.08	*	*	*	ARL ₁	14.03	15.99	*	*			
	ARL ₁ *	20.47	17.33	15.81	14.34	12.67	13.31	15.36	19.01	26.42	47.42	*	*	*	*								
(0.1, 0.1)	ARL ₁	18.55	16.37	15.25	13.96	11.68	11.25	11.82	13.17	15.35	19.11	26.43	46.43	*	*	ARL ₁	12.26	12.29	*	*			
	ARL ₁ *	18.21	15.38	14.03	12.67	10.99	11.27	12.58	14.72	18.44	25.83	47.84	*	*	*								

The asterisk (*) represents the ARL value larger than 200.

Table 5: Zero-state ARLs of different charts for the upward shift domain when $\delta = 0.5$ and $ARL_0 = 200$

		MCUSUM GBE / Paired individual CUSUM															MEWMA				
k		0.02	0.05	0.07	0.1	0.2	0.3	0.4	0.5	0.6	0.7	0.8	0.9	1	3	r		0.02	0.1	0.5	1
(τ_1, τ_2)	H	17.59	15.52	14.34	12.90	9.78	8.14	7.24	6.68	6.27	5.93	5.63	5.38	5.15	2.46	H'	5.28	10.34	23.60	29.55	
	h	19.45	16.34	14.73	12.83	9.24	7.58	6.69	6.11	5.65	5.30	5.01	4.76	4.53	1.97						
(1, 1)	ARL_0	199.84	200.75	199.55	200.01	199.64	199.96	199.32	199.72	199.88	199.48	199.75	199.96	199.68	199.82	ARL'_0	199.96	200.20	199.31	199.81	
	ARL_6	199.89	200.69	200.41	199.60	199.85	199.65	199.54	199.90	199.46	199.18	199.02	200.93	200.78	199.71						
(1.5, 1)	ARL_1	37.80	28.40	27.01	25.39	22.37	21.66	22.28	23.75	25.77	27.44	29.36	30.91	32.29	44.60	ARL'_1	23.67	22.41	36.95	46.55	
	ARL_1^*	41.19	36.79	34.15	31.53	27.56	27.01	27.73	29.52	30.76	32.38	33.66	35.39	36.52	47.11						
(2, 1)	ARL_1	16.04	14.66	13.87	12.89	10.85	9.99	9.76	9.94	10.13	10.47	10.93	11.43	11.71	16.80	ARL'_1	11.84	9.65	13.66	17.91	
	ARL_1^*	21.41	18.72	17.29	15.76	12.85	11.94	11.77	11.98	12.18	12.47	12.92	13.40	13.75	18.44						
(5, 1)	ARL_1	4.79	4.38	4.12	3.87	3.28	2.99	2.84	2.76	2.72	2.69	2.66	2.68	2.69	2.89	ARL'_1	3.58	2.78	2.70	3.02	
	ARL_1^*	6.12	5.36	5.00	4.53	3.69	3.33	3.18	3.08	3.03	2.96	2.97	2.96	2.94	3.18						
(10, 1)	ARL_1	2.68	2.49	2.39	2.25	1.99	1.86	1.79	1.75	1.72	1.71	1.70	1.68	1.67	1.68	ARL'_1	2.13	1.76	1.65	1.70	
	ARL_1^*	3.27	2.94	2.76	2.56	2.17	2.01	1.92	1.88	1.85	1.83	1.81	1.80	1.78	1.79						
(1.5, 1.5)	ARL_1	31.20	28.53	26.93	25.04	21.25	19.50	19.24	19.64	20.38	20.95	21.61	22.15	23.02	29.51	ARL'_1	23.05	19.07	25.91	30.72	
	ARL_1^*	34.47	30.16	27.79	25.29	20.68	19.27	19.41	19.80	20.25	20.90	21.74	22.48	22.87	28.69						
(2, 2)	ARL_1	16.10	14.55	13.61	12.49	10.29	9.16	8.73	8.65	8.67	8.72	8.82	8.99	9.13	11.55	ARL'_1	11.47	8.72	10.16	12.13	
	ARL_1^*	18.10	15.56	14.37	12.75	10.04	9.00	8.64	8.56	8.54	8.64	8.78	8.91	9.12	11.05						
(5, 5)	ARL_1	4.57	4.15	3.92	3.63	3.03	2.72	2.56	2.49	2.43	2.40	2.37	2.37	2.34	2.38	ARL'_1	3.34	2.52	2.31	2.43	
	ARL_1^*	5.11	4.45	4.11	3.72	3.01	2.69	2.53	2.45	2.39	2.35	2.31	2.31	2.28	2.34						
(10, 10)	ARL_1	2.48	2.30	2.19	2.08	1.83	1.70	1.64	1.59	1.58	1.56	1.55	1.54	1.53	1.50	ARL'_1	1.96	1.63	1.50	1.51	
	ARL_1^*	2.72	2.44	2.30	2.12	1.82	1.68	1.62	1.58	1.55	1.53	1.52	1.51	1.49	1.49						

Table 6: Steady-state ARLs of different charts for the upward shift domain when $\delta = 0.5$ and $ARL_0 = 200$

		MCUSUM GBE / Paired individual CUSUM															MEWMA				
(τ_1, τ_2)	k	0.02	0.05	0.07	0.1	0.2	0.3	0.4	0.5	0.6	0.7	0.8	0.9	1	3	r	H'	0.02	0.1	0.5	1
(1, 1)	ARL_0	199.41	200.41	199.92	199.28	200.52	200.01	200.17	200.31	199.67	200.17	199.39	199.53	200.25	199.41	ARL_0	200.60	200.60	200.23	199.63	200.70
	ARL_0^*	200.07	200.36	199.70	199.70	199.23	199.61	200.10	199.88	200.73	199.17	199.64	200.00	200.29	199.72						
(1.5, 1)	ARL_1	31.43	28.44	26.76	24.82	21.53	20.86	21.78	23.33	25.15	27.03	28.84	30.38	32.18	44.88	ARL_1	23.05	22.17	36.98	46.19	
	ARL_1^*	37.03	32.20	29.95	27.75	25.40	25.48	27.01	28.46	30.22	31.90	33.35	34.94	36.14	47.05						
(2, 1)	ARL_1	16.55	14.80	13.80	12.70	10.52	9.67	9.42	9.66	9.85	10.29	10.69	11.04	11.58	16.84	ARL_1	11.58	9.55	13.48	17.82	
	ARL_1^*	19.13	16.43	15.05	13.74	11.59	11.10	11.14	11.44	11.89	12.32	12.78	13.10	13.50	18.30						
(5, 1)	ARL_1	4.94	4.43	4.17	3.86	3.23	2.92	2.79	2.71	2.68	2.66	2.65	2.65	2.64	2.91	ARL_1	3.53	2.75	2.70	3.01	
	ARL_1^*	5.51	4.76	4.43	4.04	3.37	3.11	3.00	2.95	2.92	2.91	2.90	2.90	2.91	3.19						
(10, 1)	ARL_1	2.74	2.52	2.41	2.26	1.97	1.84	1.77	1.73	1.70	1.68	1.68	1.68	1.65	1.68	ARL_1	2.10	1.75	1.65	1.70	
	ARL_1^*	3.01	2.67	2.52	2.34	2.03	1.90	1.86	1.83	1.80	1.79	1.78	1.77	1.77	1.79						
(1.5, 1.5)	ARL_1	32.09	28.71	26.90	24.71	20.58	19.02	18.69	18.96	19.66	20.47	21.02	21.85	22.71	29.34	ARL_1	22.84	18.92	25.90	31.02	
	ARL_1^*	30.35	26.14	23.95	21.96	18.62	17.81	18.47	18.83	19.71	20.53	21.23	21.89	22.42	28.65						
(2, 2)	ARL_1	16.71	14.80	13.74	12.56	10.09	8.98	8.53	8.38	8.38	8.46	8.62	8.79	9.01	11.47	ARL_1	11.38	8.54	10.08	12.03	
	ARL_1^*	15.71	13.25	12.15	10.91	8.90	8.25	8.13	8.11	8.26	8.38	8.55	8.79	8.95	11.19						
(5, 5)	ARL_1	4.76	4.25	3.96	3.66	2.99	2.67	2.52	2.42	2.37	2.34	2.32	2.30	2.30	2.37	ARL_1	3.36	2.51	2.32	2.44	
	ARL_1^*	4.51	3.87	3.58	3.25	2.68	2.47	2.39	2.32	2.30	2.27	2.26	2.27	2.25	2.33						
(10, 10)	ARL_1	2.57	2.35	2.25	2.10	1.82	1.68	1.61	1.58	1.55	1.53	1.51	1.51	1.51	1.50	ARL_1	1.97	1.61	1.49	1.51	
	ARL_1^*	2.47	2.19	2.06	1.92	1.69	1.60	1.56	1.53	1.52	1.50	1.49	1.49	1.49	1.48						

Table 7: Zero-state ARLs of different charts for the hybrid shift domain when $\delta = 0.5$ and $ARL_0 = 200$

		MCUSUM GBE / Paired individual CUSUM															MEWMA				
		0.02	0.05	0.07	0.1	0.2	0.3	0.4	0.5	0.6	0.7	0.8	0.9	1	3	r	0.02	0.1	0.5	1	
(τ_1, τ_2)	k	17.59	15.52	14.34	12.90	9.78	8.14	7.24	6.68	6.27	5.93	5.63	5.38	5.15	2.46	H'	5.28	10.34	23.60	29.55	
	h	19.45	16.34	14.73	12.83	9.24	7.58	6.69	6.11	5.65	5.30	5.01	4.76	4.53	1.97						
(1, 1)	ARL ₀	199.84	200.75	199.55	200.01	199.64	199.96	199.32	199.72	199.88	199.48	199.75	199.96	199.68	199.82	ARL ₀	199.96	200.20	199.31	199.81	
	ARL ₆	199.89	200.69	200.41	199.60	199.85	199.65	199.54	199.90	199.46	199.18	199.02	200.93	200.78	199.71						
(0.8, 1.5)	ARL ₁	24.32	22.35	21.24	19.88	17.25	16.70	17.27	18.74	20.55	22.79	24.77	26.72	28.75	43.78	ARL ₁	18.45	17.54	33.92	45.71	
	ARL ₁ *	39.23	34.82	32.46	29.78	26.09	26.58	28.29	30.11	31.79	33.69	35.04	36.73	37.98	50.66						
(0.5, 2)	ARL ₁	11.96	10.79	10.20	9.42	7.89	7.21	6.97	7.02	7.22	7.49	7.76	8.10	8.52	13.93	ARL ₁	8.64	6.92	10.51	14.95	
	ARL ₁ *	20.75	18.05	16.59	14.99	12.12	11.35	11.43	11.82	12.25	12.68	13.05	13.40	13.93	18.83						
(0.2, 5)	ARL ₁	4.29	3.91	3.72	3.48	2.94	2.69	2.55	2.49	2.43	2.42	2.41	2.41	2.39	2.61	ARL ₁	3.22	2.50	2.43	2.70	
	ARL ₁ *	6.11	5.36	4.98	4.56	3.71	3.33	3.18	3.07	3.02	2.99	2.97	2.95	2.96	3.19						
(0.1, 10)	ARL ₁	2.56	2.37	2.30	2.17	1.90	1.77	1.71	1.67	1.65	1.63	1.62	1.61	1.60	1.61	ARL ₁	2.04	1.69	1.58	1.63	
	ARL ₁ *	3.26	2.93	2.76	2.56	2.18	2.02	1.93	1.87	1.84	1.82	1.81	1.80	1.79	1.81						

Table 8: Steady-state ARLs of different charts for the hybrid shift domain when $\delta = 0.5$ and $ARL_0 = 200$

		MCUSUM GBE / Paired individual CUSUM															MEWMA						
		0.02	0.05	0.07	0.1	0.2	0.3	0.4	0.5	0.6	0.7	0.8	0.9	1	3	r	H'	0.02	0.1	0.5	1		
(τ_1, τ_2)	k	19.33	16.72	15.28	13.56	9.99	8.23	7.29	6.71	6.28	5.94	5.64	5.38	5.16	2.46	5.52	10.37	23.62	29.55				
	h	21.43	17.63	15.71	13.52	9.43	7.64	6.74	6.12	5.68	5.31	5.01	4.76	4.53	1.97								
(1, 1)	ARL_0	199.41	200.41	199.92	199.28	200.52	200.01	200.17	200.31	199.67	200.17	199.39	199.53	200.25	199.41	ARL'_0	200.60	200.23	199.63	200.70			
	ARL'_0	200.07	200.36	199.70	199.70	199.23	199.61	200.10	199.88	200.73	199.17	199.64	200.00	200.29	199.72								
(0.8, 1.5)	ARL_1	24.89	22.28	20.92	19.33	16.62	16.05	16.71	18.35	20.19	22.36	24.44	26.43	28.22	43.55	ARL'_1	17.79	17.42	33.90	45.71			
	ARL'_1	34.44	29.52	27.35	25.22	23.34	24.92	27.24	29.52	31.41	32.96	34.91	36.13	37.66	50.45								
(0.5, 2)	ARL_1	12.24	10.89	10.17	9.31	7.61	6.96	6.74	6.82	7.01	7.31	7.62	7.97	8.48	13.89	ARL'_1	8.33	6.80	10.49	14.84			
	ARL'_1	17.88	15.02	13.72	12.47	10.54	10.27	10.78	11.37	11.93	12.42	12.80	13.27	13.76	18.71								
(0.2, 5)	ARL_1	4.41	3.97	3.71	3.46	2.91	2.62	2.51	2.44	2.41	2.38	2.39	2.37	2.36	2.61	ARL'_1	3.15	2.46	2.41	2.70			
	ARL'_1	5.52	4.76	4.39	4.00	3.36	3.10	3.00	2.94	2.91	2.90	2.91	2.92	2.93	3.19								
(0.1, 10)	ARL_1	2.60	2.41	2.29	2.16	1.89	1.76	1.70	1.65	1.63	1.62	1.61	1.60	1.59	1.60	ARL'_1	2.02	1.67	1.58	1.62			
	ARL'_1	3.01	2.67	2.51	2.33	2.04	1.91	1.86	1.83	1.80	1.79	1.78	1.78	1.76	1.80								

Table 9: An example of using the MCUSUM GBE chart on monitoring of patient headache relief time ($k = 0.1, H = 12.89, \delta = 0.2072$)

t	\mathbf{X}_t		C_t	\mathbf{S}_t		Q_t
	$X_{1,t}$	$X_{2,t}$		$S_{1,t}$	$S_{2,t}$	
0.				0	0	0
1.	3.4000	1.9000	0.6322	-0.0253	-0.6566	0.5322
2.	2.7000	1.8000	0.8687	-0.6683	-1.3597	0.7687
3.	5.1000	5.3000	0.5507	0.8198	1.0314	0.4507
4.	4.6000	4.4000	1.2736	1.8335	2.5354	1.1736
5.	4.3000	3.0000	1.1268	2.4636	2.6020	1.0268
6.	4.1000	3.8000	1.5699	2.9340	3.4849	1.4699
7.	4.0000	1.1000	1.1171	3.1903	1.7344	1.0171
8.	2.7000	2.4000	0.7503	2.1324	1.2605	0.6503
9.	3.1000	3.0000	0.5898	1.4968	1.3125	0.4898
10.	0.3000	0.1000	0.4877	-1.2983	-1.0076	0.3877
11.	1.6760	3.1124	1.5726	-2.8582	-0.5386	1.4726
12.	1.6438	4.2428	3.8038	-4.5223	-0.9972	3.7038
13.	0.4063	0.9595	4.3799	-7.3738	-0.7068	4.2799
14.	1.5115	4.0282	6.5283	-9.1499	0.6316	6.4283
15.	0.8929	1.6954	7.3430	-11.5279	-0.3482	7.2430
16.	0.9894	1.5942	8.0394	-13.7948	-1.4161	7.9394
17.	0.9520	5.1780	11.4010	-16.1300	1.0724	11.3010
18.	0.1621	0.3379	11.6862	-19.2319	-1.2589	11.5862
19.	1.3495	2.7953	13.0232	-21.1487	-1.1349	12.9232
20.	0.8565	1.2491	13.5593	-23.5473	-2.5469	13.4593
21.	1.1229	2.4958	14.8249	-25.6800	-2.7127	14.7249
22.	1.6223	2.5486	15.8041	-27.3138	-2.8260	15.7041
23.	0.9991	1.4017	16.3705	-29.5630	-4.0792	16.2705
24.	0.4498	1.4152	17.3119	-32.3552	-5.3131	17.2119
25.	0.0181	0.0391	17.6033	-35.5639	-7.9089	17.5033
26.	0.1179	0.2656	18.0266	-38.6603	-10.2660	17.9266
27.	1.1572	2.2237	19.0760	-40.7185	-10.6661	18.9760
28.	0.2554	0.5076	19.5967	-43.6691	-12.7730	19.4967
29.	0.7168	1.4215	20.4164	-46.1551	-13.9628	20.3164
30.	0.0828	0.1625	20.8674	-49.2651	-16.4013	20.7674

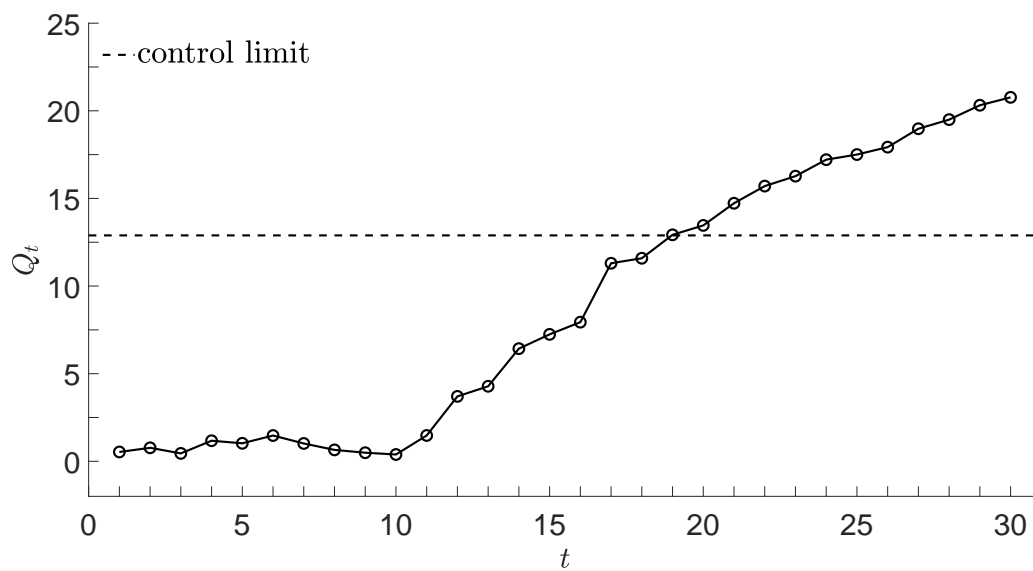


Figure 1: Monitoring procedure using the MCUSUM GBE chart ($k=0.1$, $H=12.89$, $\delta = 0.2072$)